Mutual Interference of Two Surface Cracks in a Semi-Infinite Body Due to Rolling Contact with Frictional Heating by a Rigid Roller*

Takahito GOSHIMA** and Yuuji KAMISHIMA***

This paper deals with the two-dimensional thermoelastic contact problem of a rolling rigid cylinder of specified shape, which induces effects of friction and heat generation in the contact region, moving with constant velocity in an elastic half-space containing two surface cracks located close to each other. In the present temperature analysis, the speed of the moving heat source is assumed to be much greater than the ratio of the thermal diffusivity to the contact length. The problem is solved using complex-variable techniques and is reduced to a pair of singular integral equations which are solved numerically. Numerical results of stress intensity factors are obtained for the case of two parallel cracks. The variance in interference effects on the stress intensity factors with distance between two cracks, and the effects of the frictional coefficient, the sliding/rolling ratio and the distribution of heat generation on the results are considered.

Key Words: Elasticity, Thermal Stress, Stress Intensity Factor, Rolling-Sliding Contact, Mutual Interference, Surface Crack, Frictional Heating

1. Introduction

Since the analysis of Keer and coworkers[1),(2)], a considerable amount of research[3)-(8)] on fracture mechanics has been performed in order to understand the mechanism of the rolling contact fatigue failure in railroads, gears and ball bearings. These studies, however, dealt with a single crack. In actual rolling contact fatigue failure, multiple cracks occur. Goshima and coworkers[9),(10)] first analyzed the stress intensity factors for multiple surface cracks in an elastic half-space under rolling contact. However, they only considered an isothermal case. Most rolling contacts are accompanied by frictional heat generation due to the relative slip between the two contact surfaces. Goshima and coworkers[11)-(14)] subsequently dealt with the thermoelastic rolling contact problem for a single surface crack. For the analysis of multiple cracks accompanied by frictional heating, the authors[15)] have dealt with a thermoelastic rolling contact problem with a specified contact pressure distribution. For isothermal rolling contact, the contact pressure shows a Hertzian distribution[2)]. However, Dow et al.[16)] and Burton et al.[17)] showed that the contact pressure distribution is not always Hertzian for the case of thermoelastic rolling contact. Therefore, it is more realistic, for actual thermoelastic rolling contact, to specify the shape of displacement beneath the roller instead of specifying the contact pressure distribution.

In this study, we analyze the stress intensity factors for a pair of surface cracks in an elastic half-space under rolling-sliding contact accompanied by frictional heat having either Hertzian or parabolic distribution. This thermoelastic contact is dealt with as a mixed boundary value problem with a specified displacement shape beneath the rigid roller. The crack face friction is neglected. In the present temperature analysis, it is assumed that the speed of the moving contact region is much greater than the ratio of the thermal diffusivity to the contact length (large

* Received 2nd March, 1995. Japanese original: Trans. Jpn. Soc. Mech. Eng., Vol. 50, No. 566, A (1993), pp. 2373-2380. (Received 18th March, 1993)

** Faculty of Engineering, Toyama University, 3190 Gofuku, Toyama City 930, Japan

*** Toyama Murata Corporation, 345 Ueno, Toyama City 930, Japan

Peclet number), and that the temperature distribution is not disturbed by the cracks. Numerical calculations of stress intensity factors are carried out for a pair of parallel cracks. The effects of the distance between cracks, the frictional coefficient, the slide/roll ratio and the crack angle upon mutual interference of cracks are considered numerically.

2. Problem Formulation

An elastic half-space containing a pair of surface cracks is subjected to rolling-sliding contact by a rigid roller with constant moving velocity V, as shown in Fig. 1. The surface of the half-space is specified as the displacement shape of the roller in the contact region. We call the cracks crack 1 and crack 2 in the order of contact. In the analysis, the dimensionless parameters for crack 1 or 2 are represented by subscript k (where $k=1, 2$) and are shown as

$$(x, y)=(\tilde{x}/c, \tilde{y}/c),\ (\xi_k, \zeta_k)=(\tilde{\xi}_k/c, \tilde{\zeta}_k/c),$$
$$x_k=\tilde{x}_k/c,\ x_k^*=\tilde{x}_k^*/c,\ x_0=\tilde{x}_0/c,\ y_0=\tilde{y}_0/c,$$
$$d=\tilde{d}/c,\ R=\tilde{R}/c,\ l_k=\tilde{l}_k/c,$$
$$P_e=cV/\chi_t,\ S_r=V_s/V,\ Q(x)=Q_1(\tilde{x})/Q_0,$$
$$H_0=\frac{2\alpha_0 G_0 \chi_t(1+\nu)}{K_t(1-\nu)},\ P_r=\frac{RP_0}{G_0},$$

where χ_t is thermal diffusivity, K_t is thermal conductivity, G_0 is shear modulus, ν is Poisson's ratio, α_0 is coefficient of thermal expansion, P_0 is the maximum pressure, x_0 and y_0 are the rigid displacement components of yhe roller, V_s is the sliding velocity during rolling contact, P_e is Peclet number and S_r is the slide/roll ratio. Assuming that all the work done by the friction load is transformed into heat energy, the frictional heat generation is given as $Q_1(x)=fV_sP_1(x)$, $P_1(x)$ being contact pressure and f being frictional coefficient. However in the present study, having specified the displacement shape of the roller, the contact pressure distribution $P_1(x)$ is not given, and $Q_1(x)$ cannot be determined. In the present analysis, we assume that the frictional heat generation $Q_1(x)$ is given as

$$Q_1(x)=Q_0Q(x)=fVS_rP_0Q(x), \tag{1}$$

where the distribution of heat generation $Q(x)$ is assumed to be a proper function of x.

The region outside the area of contact is assumed to be thermally insulated. Furthermore, it is assumed that the temperature distribution $T(x, y)$ is not affected by the presence of cracks. Thus, the thermal boundary conditions can be given as follows.

$$\left(\frac{\partial T}{\partial y}\right)_{y=0}=\begin{cases} fcVS_rP_0Q(x)/K_t, & |x|<1 \\ 0, & |x|>1 \end{cases} \tag{2}$$

$$(T)_{y\to-\infty}=0 \tag{3}$$

The mechanical boundary conditions on the surface and at infinity of the half-space are given as

$$\sigma_{xy}+f\sigma_{yy}=0,\ |x|<1 \tag{4}$$
$$\sigma_{yy}+i\sigma_{xy}=0,\ |x|>1 \tag{5}$$
$$U_{yy}/c=(x-x_0)^2/(2R)+y_0,\ |x|<1 \tag{6}$$
$$(\sigma_{pq})_{y\to-\infty}=0,\ (p, q=x, y), \tag{7}$$

where σ_{pq} $(p, q=x, y)$ are the stress components, U_{yy} is a vertical displacement and $i^2=-1$.

Assuming that crack-face friction is neglected, the boundary condition along the cracks may be expressed as

$$(\sigma_{\xi_k\zeta_k})_{\zeta_k=0}=0,\ 0<\xi_k<l_k,\ k=1, 2 \tag{8}$$
$$(\sigma_{\zeta_k\zeta_k})_{\zeta_k=0}=0,\ \xi_k\in\xi_{k\mathrm{op}},\ k=1, 2, \tag{9}$$

where $\xi_{k\mathrm{op}}$ is the crack face opening region of crack k.

3. Stress Analysis

In general, using Muskhelishivili's complex stress function $\Phi(z)$, $\Psi(z)$ and a thermoelastic potential ω, thermal stresses and displacements are represented as[18]

$$\sigma_{yy}+\sigma_{xx}=2\{\Phi(z)+\overline{\Phi(z)}\}-2G_0\nabla^2\omega \tag{10}$$
$$\sigma_{yy}-\sigma_{xx}-2i\sigma_{xy}=2\{z\overline{\Phi'(z)}+\overline{\Psi(z)}\}-2G_0\left(\frac{\partial^2\omega}{\partial x^2}-\frac{\partial^2\omega}{\partial y^2}+2i\frac{\partial^2\omega}{\partial x\partial y}\right) \tag{11}$$
$$2G_0(U'_{xx}/c+iU'_{yy}/c)=\chi\Phi(z)-\overline{\Phi(z)}-z\overline{\Phi'(z)}-\overline{\Psi(z)}+2G_0\left(\frac{\partial^2\omega}{\partial x^2}+i\frac{\partial^2\omega}{\partial x\partial y}\right) \tag{12}$$
$$\nabla^2\omega=\frac{1+\nu}{1-\nu}\alpha_0T(x, y), \tag{13}$$

where primes denote differentiation with respect to $z(=x+y_i)$ and.

$\nabla^2=\partial^2/\partial x^2+\partial^2/\partial y^2$, $\chi=3-4\nu$.

First, consider the thermoelastic problem of a rigid roller sliding with friction and arbitrarily distributed heat input on an uncracked half-space. The quasi-stationary temperature solution in a half-space due to a fast-moving heat source, which satisfies the boundary conditions Eqs. (2) and (3), is given as[19]

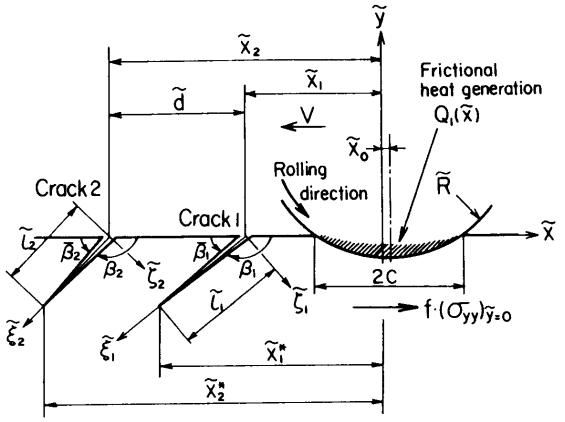

Fig. 1 Problem configuration and coordinate system

$$T(x,y)=\begin{cases}0, & -\infty<x<-1\\ \dfrac{T^*}{\sqrt{\pi P_e}}\displaystyle\int_{-1}^{x}\frac{Q(t)}{\sqrt{x-t}}e^{-Pe^2y/4(x-t)}dt, & -1<x<1\\ \dfrac{T^*}{\sqrt{\pi P_e}}\displaystyle\int_{-1}^{1}\frac{Q(t)}{\sqrt{x-t}}e^{-Pe^2y/4(x-t)}dt, & 1<x<\infty,\end{cases} \tag{14}$$

where $T^*=2fVS_rP_0c/K_t$. Substituting Eq. (14) into Eq. (13), we can easily get the solution of ω. From the known solution for thermoelastic stress and displacement, the solution to this contact problem may be obtained by application of the methods described by Muskhelishvili[18] to the boundary conditions Eqs. (4)-(7). This procedure leads immediately to the Hilbert problem, the solution of which is[11]

$$\begin{aligned}\Phi_1(z)=&2iG_0(1+if)\{z-2\gamma-X(z)\}/\{R(x+1)\}\\&+fS_rH_0P_rG_0\Big[\frac{-2i(1+if)\cos(\pi\gamma)}{\pi(x+1)}S_0(z)\\&+\frac{\cos(\pi\gamma)}{\pi^2}\int_{-1}^{1}\Big\{Q(u)-\frac{f}{\sqrt{\pi P_e}}\hat{Q}_1(u)\Big\}S_1(z;\,u)du\\&+\frac{i}{2\pi\sqrt{\pi P_e}}\int_1^{\infty}\frac{S_3(v)}{v-z}dv\Big],\end{aligned} \tag{15}$$

where

$$S_0(z)=\int_{-1}^{1}\frac{Q(t)}{X^+(t)}\Big\{1+\frac{X(z)}{t-z}\Big\}dt \tag{16}$$

$$S_1(z;u)=\int_{-1}^{1}\frac{1}{X^+(t)(t-u)}\Big\{1+\frac{X(z)}{t-z}\Big\}dt,\quad |u|<1 \tag{17}$$

$$S_3(v)=\int_{-1}^{1}Q(t)(t-v)^{-3/2}dt,\quad 1\leqq v\leqq\infty \tag{18}$$

$$X^+(t)=(1+t)^{0.5-\gamma}(1-t)^{0.5+\gamma} \tag{19}$$

$$X(z)=(z+1)^{0.5-\gamma}(z-1)^{0.5+\gamma} \tag{20}$$

$$\gamma=\frac{1}{\pi}\tan^{-1}\frac{(x-1)f}{x+1} \tag{21}$$

$$\hat{Q}_1(u)=\frac{\partial}{\partial u}\int_{-1}^{u}\frac{Q(\varepsilon)}{(u-\varepsilon)^{1/2}}d\varepsilon. \tag{22}$$

The stresses and displacements in an uncracked half-space are given as follows[18].

$$(\sigma_{yy}-i\sigma_{xy})_{\Phi_1}=\Phi_1(z)-\Phi_1(\bar{z})+(z-\bar{z})\overline{\Phi_1'(z)}-2G_0\Big(\frac{\partial^2\omega}{\partial x^2}+i\frac{\partial^2\omega}{\partial x\partial y}\Big) \tag{23}$$

$$2G_0(U'_{xx}/c+iU'_{yy}/c)_{\Phi_1}=\chi\Phi_1(z)+\Phi_1(\bar{z})-(z-\bar{z})\overline{\Phi_1'(z)}+2G_0\Big(\frac{\partial^2\omega}{\partial x^2}+i\frac{\partial^2\omega}{\partial x\partial y}\Big) \tag{24}$$

To account for the stress field caused by the crack, we consider the problem of a pair of dislocations present at the points $z=z_{0k}$ ($z_{0k}=x_k+\eta_ke^{-i\beta_k}$, $k=1,2$) in an infinite space. Then the dislocation density is defined as

$$\alpha_k=\frac{G_0\{[U_{\xi_k\xi_k}]+i[U_{\zeta_k\zeta_k}]\}e^{-i\beta_k}}{i\pi c(x+1)},\quad (k=1,2) \tag{25}$$

where $\{[U_{\xi_k\xi_k}]+i[U_{\zeta_k\zeta_k}]\}$ represents the displacement jumps. This problem is solved using the following complex potential functions[20].

$$\Phi_2(z)=\sum_{k=1}^{2}\Big\{\frac{\alpha_k}{z-z_{0k}}\Big\} \tag{26}$$

$$\Psi_2(z)=\sum_{k=1}^{2}\Big\{\frac{\bar{\alpha}_k}{z-z_{0k}}+\frac{\alpha_k\bar{z}_{0k}}{(z-z_{0k})^2}\Big\} \tag{27}$$

Then the stress representation is given by Eqs. (10)-(12), and is $\omega=0$. An additional potential Φ_3, which is required to remove the surface tractions, is conveniently written in terms of Φ_2, Ψ_2 as[18]

$$\Phi_3(z)=\begin{cases}-\bar{\Phi}_2(z)-z\bar{\Phi}_2'(z)-\bar{\Psi}_2(z), & \mathrm{Im}(z)<0\\ \Phi_2(z), & \mathrm{Im}(z)>0.\end{cases} \tag{28}$$

Then the stress representation is given by Eqs. (23) and (24), and is $\omega=0$.

The superposition of the thermoelastic contact solution (Φ_1) on the dislocation solution (Φ_2, Ψ_2 and Φ_3) does not satisfy the boundary condition Eq. (6). In order to satisfy the surface boundary conditions Eqs. (4)-(6), an additional potential must be determined in order to remove the displacement effects beneath the roller that arise due to the dislocation. This interaction potential Φ_4 was derived by Bryant et al.[2], and their result can be expressed as

$$\begin{aligned}\Phi_4(z)=&-(1+if)/2\sum_{k=1}^{2}[(\alpha_k+\bar{\alpha}_k)\{F(z;\,z_{0k})-F(z;\,\bar{z}_{0k})\}-(z_{0k}-\bar{z}_{0k})\{\bar{\alpha}_kG(z;\,\bar{z}_{0k})\\&+\alpha_kG(z;\,z_{0k})\}+(\alpha_k+\bar{\alpha}_k)\{1/X(z_{0k})-1/X(\bar{z}_{0k})\}+(z_{0k}-\bar{z}_{0k})\{\bar{\alpha}_kX'(\bar{z}_{0k})/X^2(\bar{z}_{0k})\\&+\alpha_kX'(z_{0k})/X^2(z_{0k})\}],\end{aligned} \tag{29}$$

where

$$F(z;\,z_0)=\{1-X(z)/X(z_0)\}/(z-z_0) \tag{30}$$

$$G(z;\,z_0)=\{F(z;\,z_0)+X(z)X'(z_0)/X^2(z_0)\}/(z-z_0). \tag{31}$$

Thus, using the potentials $\Phi_j(j=2,3,4)$ and Ψ_2, we can obtain the stress field for a pair of dislocations $\alpha_k(k=1,2)$. Replacing the constant α_k with distributed dislocation density $\alpha_k(\eta_k)d\eta_k$ defined along the line ξ_k of each crack, the stress due to the cracks can be obtained by integration of η_k.

Superposing these results with the thermoelastic roller solution (Φ_1), the stress solution which satisfies the boundary conditions Eqs. (2)-(7), can be obtained. With substitution of these stresses into Eqs. (8) and (9), the following singular integral equations for α_k are obtained:

$$\begin{aligned}&2e^{i\beta_k}\int_0^{l_k}\frac{\alpha_k(\eta_k)}{\xi_k-\eta_k}d\eta_k+\sum_{j=1}^{2}\int_0^{l_j}\{\alpha_j(\eta_j)K_{1k}(\xi_k,\,\eta_j)+\overline{\alpha_j(\eta_j)}K_{2k}(\xi_k,\,\eta_j)\}d\eta_j\\&=-\{(\sigma_{\zeta_k\zeta_k}-i\sigma_{\xi_k\zeta_k})_{\Phi_1}\}_{\zeta_k=0},\quad k=1,2,\end{aligned} \tag{32}$$

where

$$\begin{aligned}K_{1k}(\xi_k,\,\eta_j)=&\sum_{r=3}^{4}[\hat{\Phi}_r(z_k;\,z_{0j})+(1-e^{2i\beta_k})\overline{\Phi_r^*(z_k;\,z_{0j})}-e^{2i\beta_k}\hat{\Phi}_r(\bar{z}_k;\,z_{0j})\\&+e^{2i\beta_k}(z_k-\bar{z}_k)\overline{\Phi_r^{*\prime}(z_k;\,z_{0j})}]+(1-\delta_{kj})L_{1k}(\xi_k,\,\eta_j),\quad k,j=1,2\end{aligned} \tag{33}$$

$$K_{2k}(\xi_k,\,\eta_j)=\sum_{r=3}^{4}[\Phi_r^*(z_k;\,z_{0j})$$

$$+(1-e^{2i\beta_k})\overline{\hat{\Phi}_r(z_k\,;\,z_{0j})}-e^{2i\beta_k}\Phi_r^*(\bar{z}_k\,;\,z_{0j})$$
$$+e^{2i\beta_k}(z_k-\bar{z}_k)\overline{\hat{\Phi}_r'(z_k\,;\,z_{0j})}]$$
$$+(1-\delta_{kj})L_{2k}(\xi_k,\eta_j),\quad k,j=1,2 \tag{34}$$

$$L_{1k}(\xi_k,\eta_j)=\Phi_2^*(z_k\,;\,z_{0j})+\overline{\Phi_2^*(z_k\,;\,z_{0j})}e^{2i\beta_k}$$
$$k,j=1,2 \tag{35}$$

$$L_{2k}(\xi_k,\eta_j)=\overline{\Phi_2^*(z_k\,;\,z_{0j})}+\{z_k\overline{\Phi_2^{*\prime}(z_k\,;\,z_{0j})}$$
$$+\overline{\Psi_2^*(z_k\,;\,z_{0j})}\}e^{2i\beta_k},\quad k,j=1,2 \tag{36}$$

$$\hat{\Phi}_4(z\,;\,z_0)=-(1+if)/2\{F(z\,;\,z_0)-F(z\,;\,\bar{z}_0)$$
$$-(z_0-\bar{z}_0)G(z\,;\,z_0)+1/X(z_0)-1/X(\bar{z}_0)$$
$$+(z_0-\bar{z}_0)X'(z_0)/X^2(z_0)\} \tag{37}$$

$$\Phi_4^*(z\,;\,z_0)=-(1+if)/2\{F(z\,;\,z_0)-F(z\,;\,\bar{z}_0)$$
$$-(z_0-\bar{z}_0)G(z\,;\,\bar{z}_0)+1/X(z_0)-1/X(\bar{z}_0)$$
$$+(z_0-\bar{z}_0)X'(\bar{z}_0)/X^2(\bar{z}_0)\} \tag{38}$$

$$\hat{\Phi}_3(z\,;\,z_0)=\begin{cases}-1/(z-\bar{z}_0), & \mathrm{Im}(z)<0\\ 1/(z-z_0), & \mathrm{Im}(z)>0\end{cases} \tag{39}$$

$$\Phi_3^*(z\,;\,z_0)=\begin{cases}-(z_0-\bar{z}_0)/(z-z_0)^2, & \mathrm{Im}(z)<0\\ 0, & \mathrm{Im}(z)>0\end{cases} \tag{40}$$

$$\Phi_2^*(z\,;\,z_0)=1/(z-z_0) \tag{41}$$

$$\Psi_2^*(z\,;\,z_0)=\bar{z}_0/(z-z_0)^2 \tag{42}$$

$$\delta_{kj}=1(k=j),\ 0(k\neq j),\qquad z_k=x_k+\xi_k e^{-i\beta_k}. \tag{43}$$

4. Numerical Calculations and Stress Intensity Factors

Equation (32) was solved numerically using the piecewise quadratic method of Gerasoulis[21]. The singularity at the intersection of the crack and the free surface was assumed to be on the order of less than 0.5. This behavior was approximated numerically when $\hat{a}_k(-1)=0$, where $\hat{a}_k(\hat{\eta}_k)$ is defined as

$$a_k(\eta_k)=\frac{G_0\hat{a}_k(\hat{\eta}_k)e^{-i\beta_k}}{R(1-\hat{\eta}_k^2)^{1/2}},\qquad \hat{\eta}_k=\frac{2\eta_k}{l_k}-1. \tag{44}$$

Let us divide the interval $[-1,1]$ into $2N_k$ equal parts. We define the nodal points as $\hat{\eta}_{k,n}=-1+(n-1)/N_k$ ($n=1\sim 2N_k+1$), and use the Lagrange interpolation formula for three nodal points in the approximation. Setting the collocation points as $\hat{\xi}_{k,r}=\hat{\eta}_{k,r}+1/2N_k$ ($r=1\sim 2N_k$), Eq. (32) reduces to the simultaneous linear algebraic system of $(2N_1+2N_2)$ equations for $\hat{a}_k(\hat{\eta}_{k,n})$. Using these solutions, the stress intensity factors for crack k are given as

$$K_1-iK_{II}=\frac{G_0}{R}\pi\sqrt{2cl_k}\,\hat{a}_k(1),\quad k=1,2. \tag{45}$$

In carrying out the numerical calculations, it was necessary to determine iteratively the degree of crack opening for a given set of parameters. Iteration was performed under the condition of the absence of overlap of the material. First, the numerical solution was obtained for a completely open crack ($\xi_k^{op}: 0<\xi_k<l_k$ in Eq. (9)). The resulting crack opening displacement was checked by Eq. (25), and if overlap was found as $U_{\zeta_k\zeta_k}<0$, partial crack closure was approximated by setting $Re\{a_k(\eta_{k,n})\}=0$ for that portion of the crack where overlap occurred. Then the procedure was repeated for the partially closed crack and results were verified. This method generally converged within three iterations. For the number of collocation points, a good accuracy was obtained for $N_k=10$.

Numerical calculations were carried out for parallel cracks ($\beta_1=\beta_2$) with equal length ($l_1=l_2=0.1$), $P_e=100$ and $H_0=1.0$. All of the results are shown as the dimensionless stress intensity factors K_I^* and K_{II}^* as follows.

$$K_I^*-iK_{II}^*=\frac{R}{G_0\sqrt{c}}\{K_I-iK_{II}\} \tag{46}$$

In Eq. (1), the heat input distribution $Q(x)$ is equal to the contact pressure distribution $P(x)=(\sigma_{yy})_{y=0}/P_0$. However, in the present analysis $P(x)$ is not given. Therefore, $Q(x)$ is assumed to have either a Hertzian or a parabolic distribution, as shown in Fig. 2.

Figure 3 shows the contact pressure distribution calculated using $\Phi_1(z)$ under the condition of $Q(x)$ being Hertzian and parabolic distributions for the case of frictional coefficient $f=0.2$, for three slide/roll ratios: $S_r=0, 0.1, 0.7$. The contact pressure has an approximately Hertzian distribution for small slide/roll ratio and an approximately parabolic distribution for large slide/roll ratio (for great heat generation).

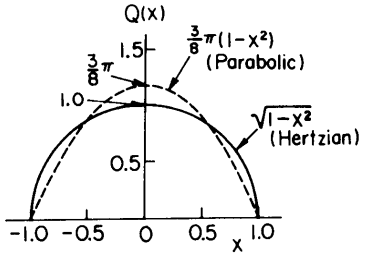

Fig. 2 Heat input distribution

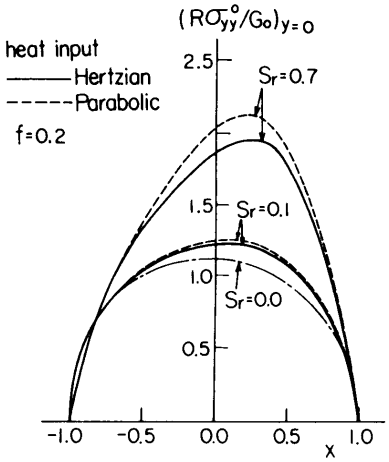

Fig. 3 Contact pressure distribution

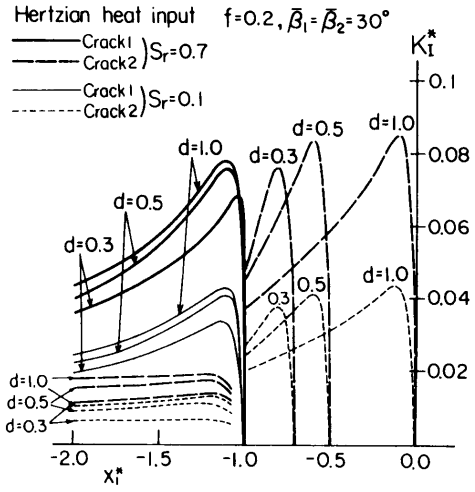

Fig. 4 Interference effects on the variation of mode I stress intensity factors under Hertzian heat input

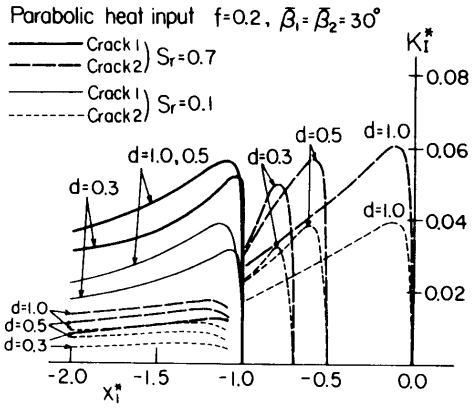

Fig. 5 Interference effects on the variation of mode I stress intensity factors under parabolic heat input

The results are not greatly affected by the difference in $Q(x)$.

Figures 4 and 5 show the numerical results of mode I stress intensity factors K_I of each crack as functions of the crack location over a complete loading cycle for Hertzian and parabolic cases. These results are shown for the cases of $f=0.2$, $\bar{\beta}_k=30°$, $S_r=0.7, 0.1$ and $d=1.0, 0.5, 0.3$. Contrary to the previous results[13]-[15], K_I for both cracks increases with an increase of S_r. This tendency is considered to be a result of the large contact thermal stresses occurring beneath the roller due to the increasing thermal effect (large S_r), and the large crack opening traction arising with those thermal stresses. The values of K_I decrease with the approach of cracks due to the mutual interference effect. The interference effects are not greatly influenced by the value of S_r, or by the difference between Hertzian and parabolic heat distributions.

Figures 6 and 7 show the mode II stress intensity

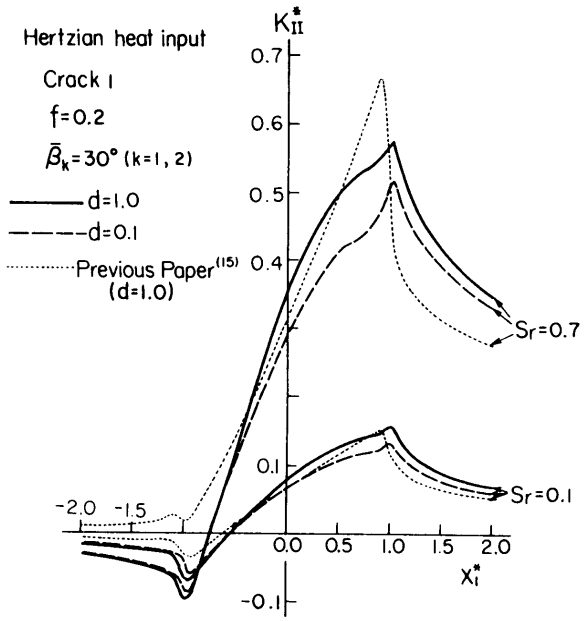

Fig. 6 Interference effects on the variation of mode II stress intensity factors for crack 1 under Hertzian heat input

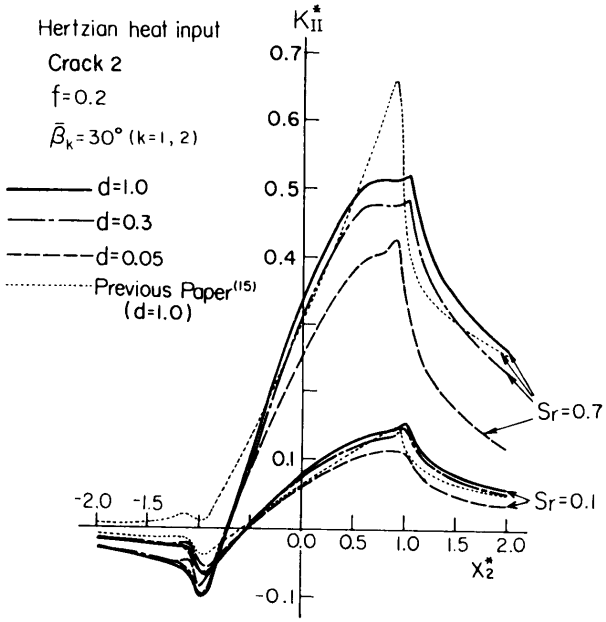

Fig. 7 Interference effects on the variation of mode II stress intensity factors for crack 2 under Hertzian heat input

factors K_{II} of crack 1 and crack 2, respectively, as functions of the crack location under Hertzian heat distribution. Figures 8 and 9 show the variation of K_{II} for crack 1 and crack 2, respectively, under parabolic heat distribution. These results are for the cases of $f=0.2$, $\bar{\beta}_k=30°$, $S_r=0.7, 0.1$ and $d=1.0, 0.1$. From these figures, we can see that K_{II} attains a positive maximum at about $x_1^*=1$ and $x_2^*=1$ ($x_k^*=1$ corresponds

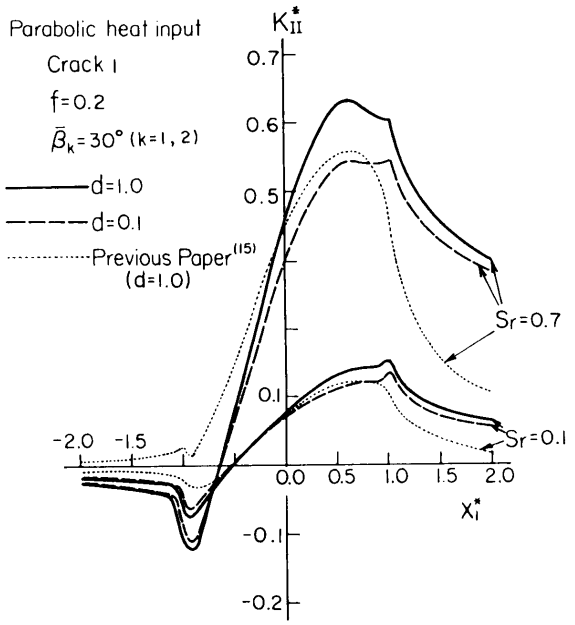

Fig. 8 Interference effects on the variation of mode II stress intensity factors for crack 1 under parabolic heat input

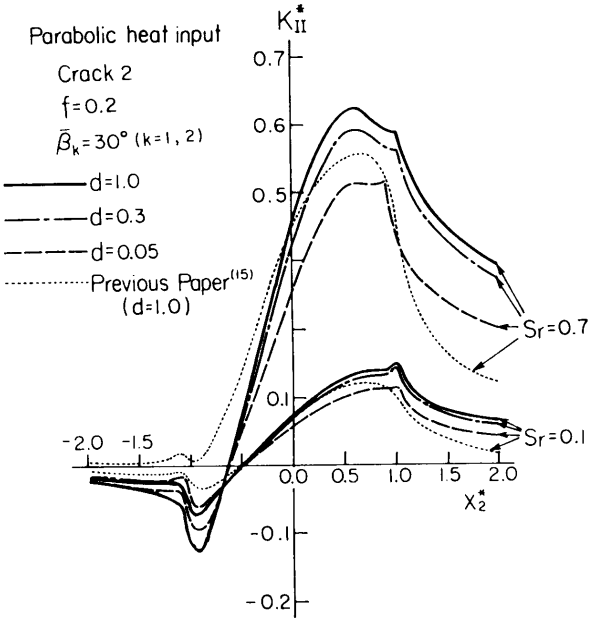

Fig. 9 Interference effects on the variation of mode II stress intensity factors for crack 2 under parabolic heat input

to the crack tip being directly beneath the right edge of the contact region) for Hertzian heat distribution. For the parabolic case, when $S_r=0.7$, K_{II} attains a positive maximum at about $x_1^*=0.5$ and $x_2^*=0.5$ (the crack tip being in the contact region). In these figures (Figs. 6 - 9), the results from a previous paper[15] (under the same contact pressure distribution as that of $Q(x)$ in Fig. 2) are also shown by the dotted line for

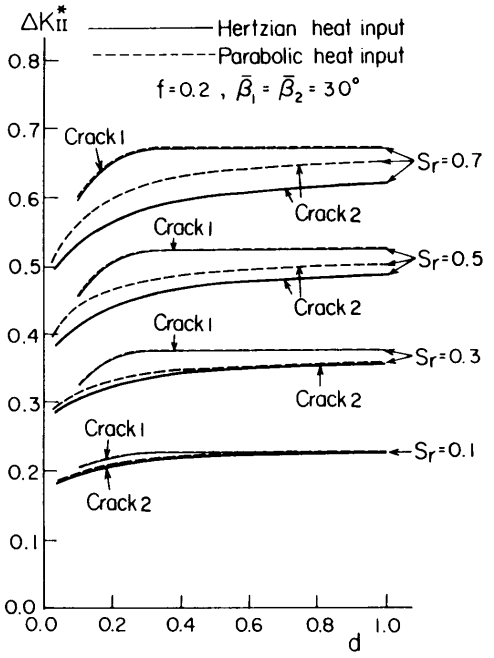

Fig. 10 Interference effects on the range of mode II stress intensity factor ΔK_{II} under Hertzian and parabolic heat inputs for various values of slide/roll ratio

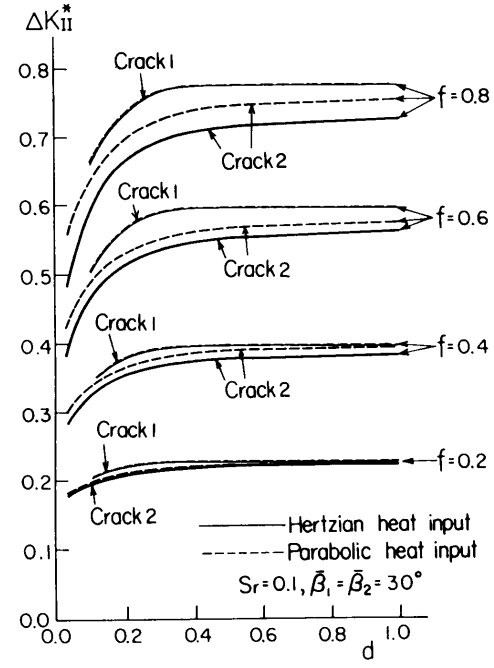

Fig. 11 Interference effects on the range of mode II stress intensity factor ΔK_{II} under Hertzian and parabolic heat inputs for various values of frictional coefficients

reference. In the case of Hertzian distribution (in Figs. 6 and 7), the present results for $S_r=0.1$ almost agree with the previous results; however, for $S_r=0.7$, the two results are not in agreement with each other.

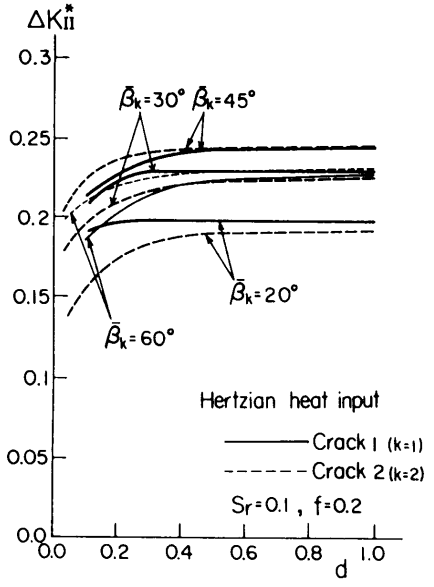

Fig. 12 Interference effects on the range of mode II stress intensity factor ΔK_{II} under Hertzian heat input for various crack inclination angles

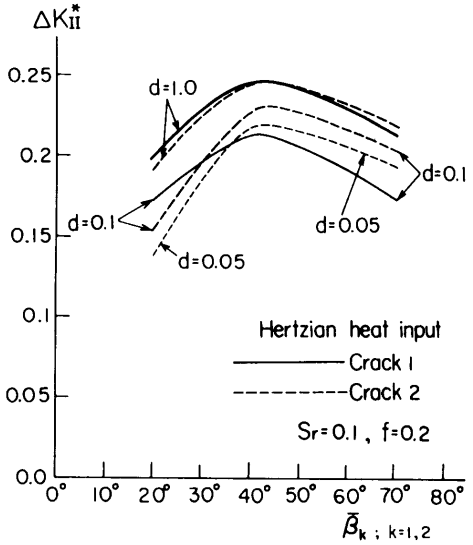

Fig. 13 Variation of the range of mode II stress intensity factor ΔK_{II} as a function of crack inclination angle under Hertzian heat input for various values of distance between the cracks

In the case of parabolic distribution (in Figs. 8 and 9), the present results for $S_r=0.7$ are qualitatively similar to the previous results. Moreover, from these figures, we can evaluate the stress intensity factor range $\Delta K_{II}=(K_{II})_{max}-(K_{II})_{min}$, the results of which are shown in Figs. 10 and 11 as functions of the distance d between the cracks. From these figures, we can recognize the effect of mutual interference of the cracks; that is, the values of K_{II} and ΔK_{II} decrease with decreasing distance between the cracks, and this tendency is more marked for a large slide/roll ratio (up to $S_r=0.7$) and large frictional coefficient (up to $f=0.8$). However, interference effects are not greatly influenced by the difference between Hertzian and parabolic heat distributions. The values of ΔK_{II} for crack 1 are always larger than the value for crack 2. The values of ΔK_{II} for crack 1 are not influenced by the difference between Hertzian and parabolic heat distributions. However, for the case of crack 2, the results for the parabolic case are always larger than those for the Hertzian case, and this tendency is more marked for large slide/roll ratio and large frictional coefficient.

Finally, in order to investigate the effects of the crack angle $\bar{\beta}_k$ on the stress intensity factors and on their mutual interference, the numerical results of ΔK_{II} are shown in Fig. 12 as functions of the distance d between the cracks at four values of $\bar{\beta}_k$ for the case of $S_r=0.1$, $f=0.2$ and Hertzian heat distribution. From this figure, we can see that the interference effects for crack 1 become more marked with increasing $\bar{\beta}_1$, and the interference effects for crack 2 become more marked with decreasing $\bar{\beta}_2$. Figure 13 shows ΔK_{II} as a function of crack angle $\bar{\beta}_k$ at $d=1.0$, 0.1 and 0.05. From this figure, we can see that ΔK_{II} attains a maximum at about $\bar{\beta}_k=40°$ independent of the crack distance d.

5. Conclusions

We analyzed the stress intensity factors for a pair of surface cracks due to rolling-sliding contact by a rigid roller with frictional heat generation. From numerical examples of the stress intensity factors for parallel cracks with equal length, the following conclusions can be drawn.

(1) In the present numerical examples, magnitudes of mode I and mode II stress intensity factors decrease with decreasing distance between the two cracks due to the mutual interference by the cracks.

(2) The interference effects on the mode II stress intensity factors become stronger with increasing magnitude of the slide/roll ratio or frictional coefficient; however, these effects are not greatly influenced by the difference in the heat distribution. The interference effects on the mode I stress intensity factors are not greatly influenced by the slide/roll ratio or the difference in the heat distributions.

(3) In the present numerical examples, when the crack inclination angle is about 40° the amplitude of the mode II stress intensity factor range attains a maximum.

(4) The contact pressure for an isothermal contact problem has a Hertzian distribution. However, the contact pressure distribution for a thermoelastic

contact problem is different from a Hertzian shape and is an approximately parabolic configuration.

Acknowledgment

The authors wish to thank Professor L. M. Keer of Northwestern University for his helpful suggestions.

References

(1) Keer, L. M. and Bryant, M. D., A Pitting Model for Rolling Contact Fatigue, Trans. ASME J. Lubr. Technol., Vol. 105 (1983), p. 198.

(2) Bryant, M. D., Miller, G. R. and Keer, L. M., Line Contact Between a Rigid Indenter and a Damaged Elastic Body, Q. J. Mech. Appl. Math., Vol. 37 (1984), p. 467.

(3) Hearle, A. D. and Johnson, K. L., Mode II Stress Intensity Factors for a Crack Parallel to the Surface of an Elastic Half-Space Subjected to a Moving Point Load, J. Mech. Phys. Solids, Vol. 33, No. 1 (1985), p. 61.

(4) Sheppard, S., Barber, J. R. and Comninou M., Short Subsurface Cracks under Conditions of Slip and Stick Caused by a Moving Compressive Load, Trans. ASME, J. Appl. Mech., Vol. 52 (1985), p. 811.

(5) Murakami, Y., Kaneta, M. and Yatsuzuka, H., Analysis of Surface Crack Propagation in Lubricated Rolling Contact, ASLE Trans., Vol. 28 (1985), p. 60.

(6) Kaneta, M., Murakami, Y. and Yatsuzuka, H., Mechanism of Crack Growth in Lubricated Rolling/Sliding Contact, ASLE Trans., Vol. 28 (1985), p. 407.

(7) Kaneta, M., Murakami, Y. and Yatsuzuka, H., Effects of Oil Pressure on Surface Crack Growth in Rolling/Sliding Contact, Tribology International, Vol. 20 (1987), p. 210.

(8) Bower, A. F., The Effects of Crack Face Friction and Trapped Fluid on Surface Initiated Rolling Contact Fatigue Cracks, Trans. ASME, J. Tribol., Vol. 110 (1988), p. 704.

(9) Goshima, T., Miyao, K. and Kamishima, Y., Mutual Interference of Two Surface Cracks in a Semi-Infinite Body Due to a Rolling Contact, Trans. Jpn. Soc. Mech. Eng., (in Japanese), Vol. 57, No. 533, A (1991), p. 19.

(10) Goshima, T., Stress Intensity Factors of Multiple Surface Cracks on a Semi-Infinite Body due to Rolling-Sliding Contact, Trans. Jpn. Soc. Mech. Eng., (in Japanese), Vol. 58, No. 547, A (1992), p. 386.

(11) Goshima, T. and Keer, L. M., Thermoelastic Contact Between a Rolling Rigid Indenter and a Damaged Elastic Body, Trans. ASME, J. Tribol., Vol. 112 (1990), p. 382.

(12) Goshima, T., Hanson, M. T. and Keer, L. M., Three-Dimensional Analysis of Thermal Effects on Surface Crack Propagation in Rolling Contact, J. Thermal Stresses, Vol. 13 (1990), p. 237.

(13) Goshima, T. and Keer, L. M., Stress Intensity Factors of a Surface Crack in a Semi-Infinite Body due to Rolling-Sliding Contact and Frictional Heating, Trans. Jpn. Soc. Mech. Eng., (in Japanese), Vol. 56, No. 532, A (1990), p. 2567.

(14) Goshima, T. and Miyao, K., Stress Intensity Factors of a Surface Crack in a Semi-Infinite Body due to Rolling-Sliding Contact and Transient Heating, Trans. Jpn. Soc. Mech. Eng., (in Japanese), Vol. 58, No. 547, A (1992), p. 393.

(15) Goshima, T. and Kamishima, Y., Mutual Interference of Multiple Surface Cracks Due to Rolling Sliding Contact with Frictional Heating, JSME Int. J., Ser. A, Vol. 37, No. 3, (1994), p. 216.

(16) Dow, T. A., Stockwell, R. D. and Kannel, J. W., Thermal Effects in Rolling/Sliding EHD Contacts: Part 1 - Experimental Measurements of Surface Pressure and Temperature, Trans. ASME, J. Tribol., Vol. 109 (1987), p. 503.

(17) Burton, R. A., Kilaparti, S. R. and Nerlikar, V., A Limiting Stationary Configuration with Partially Contacting Surface, Wear, Vol. 24 (1973), p. 199.

(18) Muskhelishvili, N. I., Some Basic Problems in the Mathematical Theory of Elasticity, (1954), 4th Ed. Noordhoff.

(19) Ling, F. F. and Mow, V. C., Surface Displacement of a Convective Elastic Half-Space Under an Arbitrarily Distributed Fast-Moving Heat Source, Trans. ASME, J. Basic Eng., Vol. 87, (1965), p. 729.

(20) Dundurs, J., Mathematical Theory of Dislocations, (1975), p. 70, ASME Publication.

(21) Gerasoulis, A., The Use of Piecewise Quadratic Polynomials for the Solution of Singular Integral Equations of Cauchy Type, Comput. Math. Applics., Vol. 8 (1982), p. 15.

(22) Azarkhin, A., Barber, J. R. and Rolf, R. L., Combined Thermal-Mechanical Effects in Frictional Sliding, Key Engineering Materials, Vol. 33 (1989), p. 135.

(23) Hills, D. A. and Barber, J. R., Steady Motion of an Insulating Rigid Flat Ended Punch Over a Thermally Conducting Half-Plane, Wear, Vol. 102 (1985), p. 15.